BMC Plant Biology

RESEARCH Open Access

Comparative organelle genome analysis of the sister genera *Ceratocephala* and *Myosurus* (Ranunculaceae) reveals fast evolutionary rates in arid and aquatic environments

Jing Long[1,2,3], Wen-Chuang He[4], Xu-Ping Zhou[1,2,3], Guan-Long Cao[1,2,3], Huan-Wen Peng[1,2,3], Tatyana V. Erst[5,6], Andrey S. Erst[7], Wei Wang[1,2,3*] and Kun-Li Xiang[1,3*]

Abstract

Background Longer branches in phylogenetic trees usually correspond to accelerated evolutionary rates. However, little is known about the potential correlation between accelerated evolution rates of organisms and their adapation to novel environments. Here, we sampled representative species of Ranunculeae in different habitats, including two xerophytic *Ceratocephala* species, two hydrophytic *Myosurus* species, and six mesophytic species from other four genera within the tribe. By an integration of phylogenomic, comparative genomic, and evolutionary rate analyses, we identified fast-evolving genes (FSGs) of organelle genomes in *Ceratocephala* and *Myosurus* and explored their relationships with adaptation to dry and aquatic habitats, respectively.

Results The *Ceratocephala-Myosurus* clade originated at 33.01 Ma and began to diversify at 24.43 Ma. A total of nine plastid FSGs (*ndhB*, *ndhD*, *rpoB*, *rpoC1*, *rps3*, *rps7*, *rps11*, *ycf1*, *ycf4*) and two mitochondrial FSGs (*ccmFC*, *nad6*) were identified as shared by *Ceratocephala* and *Myosurus*. *Ceratocephala* has four unique plastid FSGs (*rps4*, *petD*, *psbH*, *rpl22*) and two unique mitochondrial FSGs (*ccmB*, *nad4*); *Myosurus* has three unique plastid FSGs (*ndhA*, *psbC*, *rpl32*) and one unique mitochondrial FSG (*atp1*). The predicted protein structure of *ycf1* is obviously different among *Ceratocephala*, *Myosurus*, and *Ranunculus*. The predicted protein structures of *rps4* and *ccmFC* in *Ceratocephala* markedly differ from those in *Ranunculus*.

Conclusions Plastid (*rpo-*, *rps-*, *rpl-*) and mitochondrial (*nad-*, *ccm-*) genes constitute the predominant functional categories within the FSGs, implying that they may play an important role in adaptation to specific habitats. The *Ceratocephala*-specific six FSGs and predicted protein structural changes of *ycf1*, *rps4* and *ccmFC* may be related to the adaptation of this genus to dry habitats in the late Oligocene. The *Myosurus*-specific four FSGs and predicted protein structural change of *ycf1* may be associated with the adaptation of this genus to aquatic habitats. These findings

*Correspondence:
Wei Wang
wangwei1127@ibcas.ac.cn
Kun-Li Xiang
kunlixiang@ibcas.ac.cn

Full list of author information is available at the end of the article

suggest that the increases in evolutionary rates and predicted protein structural changes of organelle genes may facilitate organisms to adapt specific habitats.

Keywords Evolutionary rates, Longer branches, Organelle genomes, Phylogenomics, Ranunculaceae

Background

Adaptive evolution is a major biological theme in the genomics era, and evolutionary rate represents one of its core research topics [1, 2]. Molecular evolutionary rates are extremely heterogeneous across lineages, even among closely related taxa [3, 4]. Faster molecular evolutionary rates may enable organisms to invade novel habitats. Fast-evolving organisms can exhibit greater environmental tolerances [5]. Therefore, the differences in evolutionary rates are particularly pronounced among taxa occupying distinct habitats [5, 6]. For example, cold-responsive genes in *Cardamine resedifolia* (Brassicaceae) at high altitudes have accelerated evolutionary rates compared to those in *C. impatiens* at low altitudes [7]. However, few studies have been devoted to explore the evolutionary rates of angiosperms inhabiting dry and aquatic habitats in a phylogenetic framework.

Organelle genomes are the most frequently used sources of genetic data for reconstructing the phylogeny of plant groups and studying molecular evolutionary rates [8–10]. Organelle genomes, including the plastid genome (plastome) and mitochondrial genome (mitogenome), originated from endosymbiotic events, and are independent genetic elements located in the cytoplasm, which are generally smaller and more accessible than nuclear genomes [11]. Plastome plays an essential role in the photosynthesis of green plants, and its protein-coding genes can be categorized into seven functional groups: plastid NADH dehydrogenase-like complex (*nad*), photosynthesis-related (*psa*, *psb*), plastid-encoded RNA polymerase genes (*rpo*), plastid ATP synthase genes (*atp*), cytochrome b_6f (Cytb_6f) complex (*pet*), ribosomal protein genes (*rps*, *rpl*), and others [12]. Mitogenome encodes essential components of the electron transport chain, playing an important role in cellular respiration and ATP production, and its protein-coding genes can be categorized into six functional groups: mitochondrial NADH dehydrogenase-like complex genes (*nad*), mitochondrial ATP synthase genes (*atp*), cytochrome b_6f (Cytb_6f) complex genes (*ccm*), ribosomal protein genes (*rps*, *rpl*), mitochondrial cytochrome coxidase genes (*cox*), and others [13]. For organelle genomes, molecular evolutionary rates exhibit functional heterogeneity among genes. For example, in Geraniaceae plastomes, *rpo-*, *rps-*, and *rpl-* genes have faster evolutionary rates than other plastid genes [8]; for mitochondrial genes in Ajugoideae (Lamiaceae), *nad2* shows a typically slow rate, while *atp6*, *ccmC* and *rps12* exhibit accelerated rates [14]. Due to the functional characteristics of plastid and mitochondrial genes, the genes with fast evolutionary rates may be related to the adaptation of angiosperms to specific habitats. However, whether fast-evolving genes (FSGs) of organelle genomes in angiosperms adapting to different habitat exhibit universal or specific function remains unknown.

Ranunculeae, the largest tribe in the angiosperm family Ranunculaceae, consists of 19 genera and *ca.* 650 species [15, 16]. Most genera of this tribe grow in mesophytic habitats except *Ceratocephala*, *Myosurus* and some species of *Ranunculus* [15]. *Ceratocephala* is mainly distributed in the dry areas of Central Asia (three or four species) and New Zealand (one species; Fig. S1). *Myosurus* contains *ca.* 15 species and is mainly distributed in wet or seasonally wet areas of all continents (Fig. S1). Phylogenetic analyses indicate that within the Ranunculeae, xerophytic *Ceratocephala* and hydrophytic *Myosurus* formed a clade, which is sister to the clade containing *Laccopetalum*, *Krapfia*, and *Ranunculus* [16–19]. The phylogram of the plastomic data shows the branches of *Ceratocephala* and *Myosurus* was longer than other Ranunculeae [19], suggesting that these two genera might have faster molecular evolution rates [20, 21]. Thus, Ranunculeae provides an opportunity to study the relationship between fast molecular evolution of organelle genes and the adaptation to dry and aquatic habitats.

In this study, we sequenced plastid and mitochondrial genes of 11 species of Ranunculeae and one species of Anemoneae using the genome-skimming technique. We performed phylogenetic analyses and estimated molecular evolutionary rates using mitochondrial and plastid genomic data separately. Within the dated phylogenetic framework, we then identified FSGs of organelle genomes and predicted their protein structures of xerophytic *Ceratocephala*, hydrophytic *Myosurus*, and mesophytic *Ranunculus*. These analyses will advance our understanding about the potential relationships between the accelerated evolution of organelle genes of organisms and their adaptation to arid and aquatic environments.

Results

Phylogenetic analysis

We performed high-quality gene annotation for the 11 plastomes of Ranunculeae (Table S1), and identified 78 plastid (pt) protein-coding genes. *Ceratocephala* plastome has all 78-pt genes, while *Myosurus* plastome has 76-pt genes owing to lacking *clpP* and *rps16* (Fig. S2; Table S2). In 40 mitochondrial (mt) protein-coding genes of Ranunculeae, we only obtained 25-mt genes for

Ceratocephala and 27-mt genes for *Myosurus*, respectively (Fig. S2; Table S3).

We performed phylogenetic analyses using 78-pt gene dataset and 40-mt gene dataset, separately. The topology of Ranunculeae phylogeny generated based on 78-pt gene dataset is nearly identical with the 40-mt gene dataset, but the former received higher support (Figs. 1a and b). Based on the two datasets, *Ceratocephala* and *Myosurus* formed a clade with strong support (BS = 100%), sister to *Ranunculus* (BS = 100%). The monophyly of each of *Ceratocephala* and *Myosurus* is strongly support.

Divergence time estimation

Molecular dating was performed based on the 78-pt gene dataset (Fig. S3). The stem and crown group ages of Ranunculeae were estimated at 67.79 Ma [95% highest posterior density (HPD): 60.53–70.36 Ma] and 48.6 Ma (95% HPD: 42.03–55.59 Ma), respectively. The stem group age of *Ceratocephala-Myosurus* clade was estimated at 33.01 Ma (95% HPD: 25.26–42.6 Ma). The split between *Ceratocephala* and *Myosurus* was at 24.43 Ma (95% HPD: 23.06–31.08 Ma). *Ceratocephala* and *Myosurus* became differentiated at 0.48 Ma (95% HPD: 0.21–4.87 Ma) and 1.35 Ma (95% HPD: 0.04–1.6 Ma), respectively.

Ancestral habitat reconstruction

Based on species occurrence records, as well as annual precipitation variable and aridity index that we extracted (Table S1), *Ceratocephala* grows in arid environments, while *Myosurus* inhabits in humid environments. Our ancestral habitat reconstruction indicates that mesophytic habitat is the ancestral state in Ranunculeae (Fig. S4). The most recent common ancestor of *Ceratocephala* and *Myosurus* also occurred in mesophytic environments. The most recent common ancestors of *Ceratocephala* and *Myosurus* are xerophytic and hydrophytic, respectively.

Evolutionary rate analysis

To identify organelle FSGs in *Ceratocephala* and *Myosurus*, we used the likelihood ratio test to calculated the ω values (dN/dS, non-synonymous substitution rates/synonymous substitution rates) of organelle genes in *Ceratocephala*, *Myosurus*, and other *Ranunculus.* For 77 of 78-pt genes, the two-ratio model (m2), assuming that the foreground branch has evolved under a different rate (alternative hypothesis), was identified as best-fit to *Ceratocephala*, *Myosurus*, and other Ranunculeae. For the photosystem II factor gene (*psbJ*), the one-ratio model (m0), assuming that all branches have been evolving at the same rate (null hypothesis), was identified as best-fit (Table S4). The ω values of 31-pt genes in *Ceratocephala* and 32-pt genes in *Myosurus* were higher than those in *Ranunculus* (Fig. 2; Table S4). Moreover, nine plastid genes, including two NADH dehydrogenase-like complex genes (*ndhB*, *ndhD*), two plastid-encoded RNA polymerase genes (*rpoB*, *rpoC1*), three ribosome small subunit genes (*rps3*, *rps7*, *rps11*), an unknown function gene (*ycf1*), and a photosystem assembly factor gene (*ycf4*), evolved faster in both *Ceratocephala* and *Myosurus* with p-value < 0.05 (Figs. 2 and 3; Table S4). Four

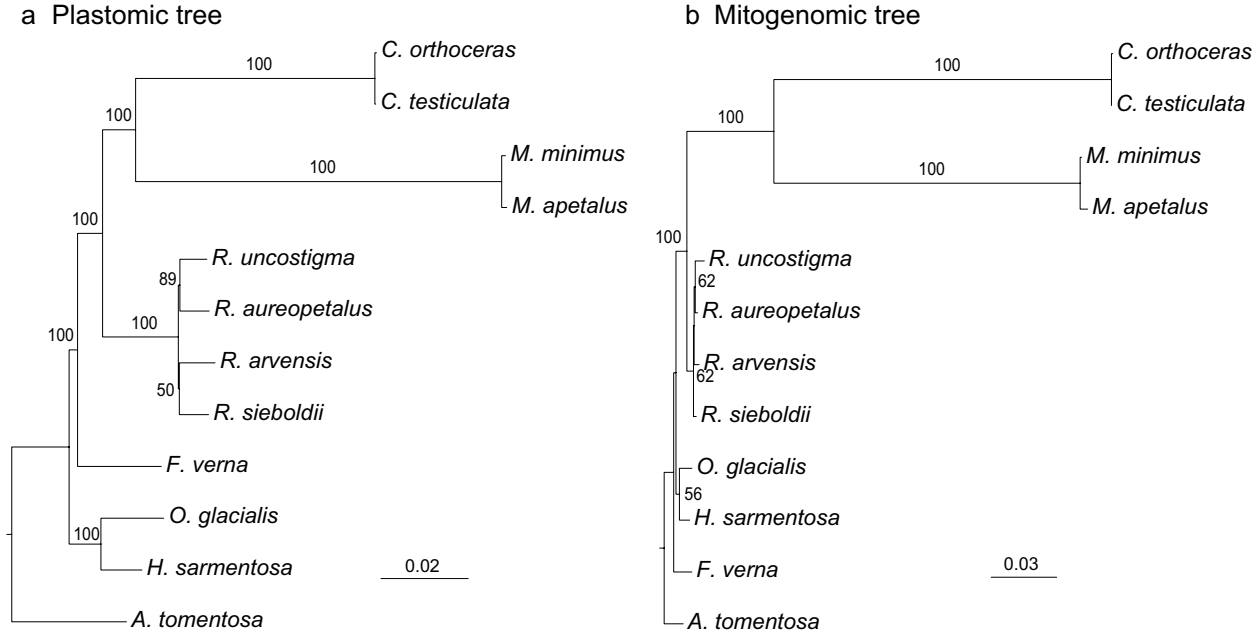

Fig. 1 Phylogeny of Ranunculeae. **a** ML tree inferred from the 78-pt gene data. **b** ML tree inferred from 40-mt gene data. Numbers above branches are bootstrap values (≥ 50%)

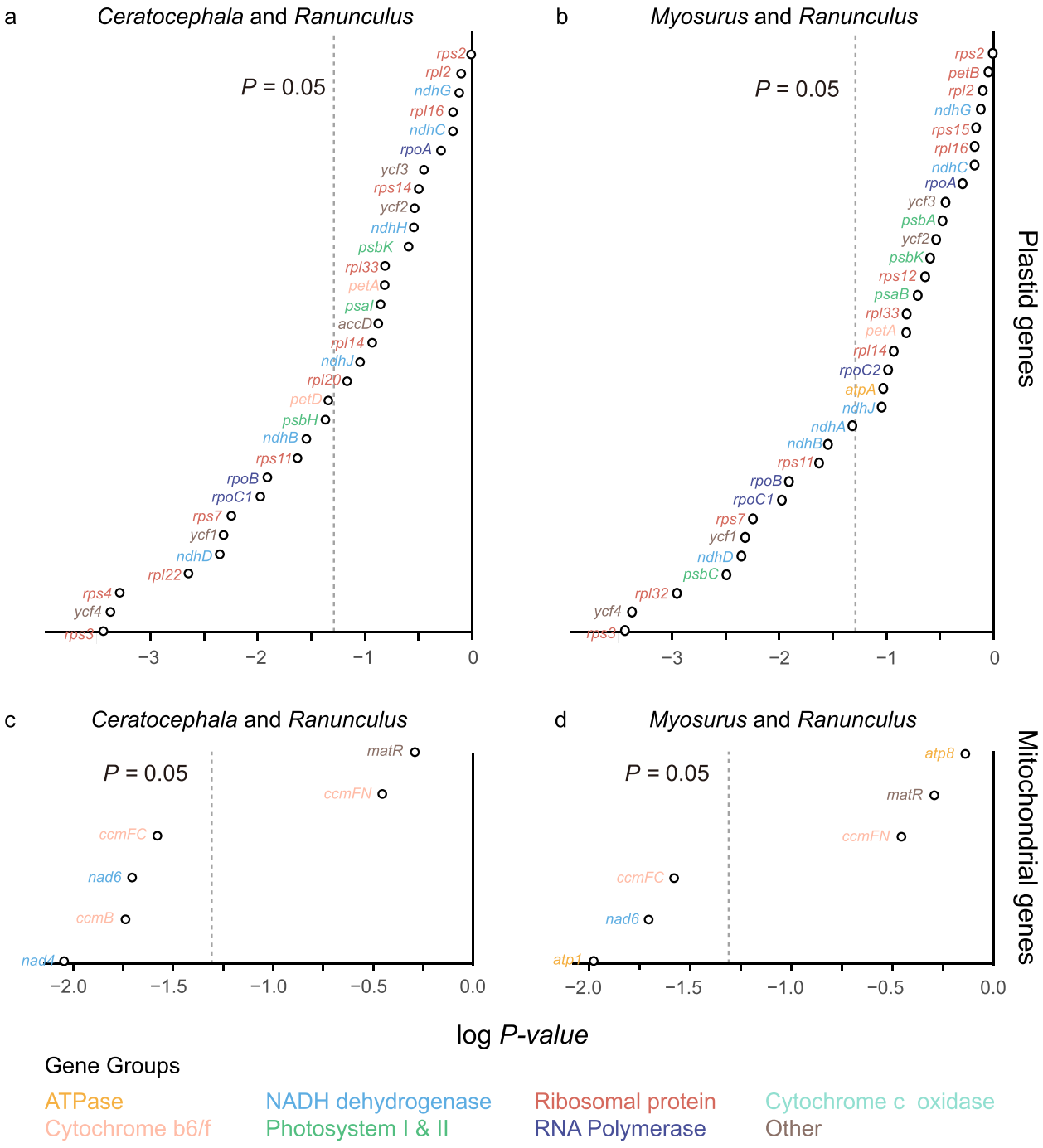

Fig. 2 Plot of ranked log *P*-values for selected genes from the likelihood ratio test. The vertical line shows a *P*-value cut-off, and genes appearing to the left of the vertical line have a significantly higher ω value. **a** Ranked log *P*-values of plastid genes with significantly higher ω values in *Ceratocephala* against *Ranunculus*. **b** Ranked log *P*-values of plastid genes with significantly higher ω values in *Myosurus* against *Ranunculus*. **c** Ranked log *P*-values of mitochondrial genes with significantly higher ω values in *Ceratocephala* against *Ranunculus*. **d** Ranked log *P*-values of mitochondrial genes with significantly higher ω values in *Myosurus* than in *Ranunculus*

FSGs, including a ribosome small subunit gene (*rps4*), a Cytochrome b_6f complex gene (*petD*), a photosynthesis-related gene (*psbH*), and a ribosome large subunit gene (*rpl22*), were identified in *Ceratocephala*. Three FSGs, including a NADH dehydrogenase-like complex gene (*ndhA*), a photosynthesis-related gene (*psbC*), and a ribosome large subunit gene (*rpl32*), were identified in *Myosurus* (Figs. 2 and 3; Table S4).

We excluded 10 mt-genes that were missing in both *Ceratocephala* and *Myosurus*. For 28 of 30 mt-genes, the

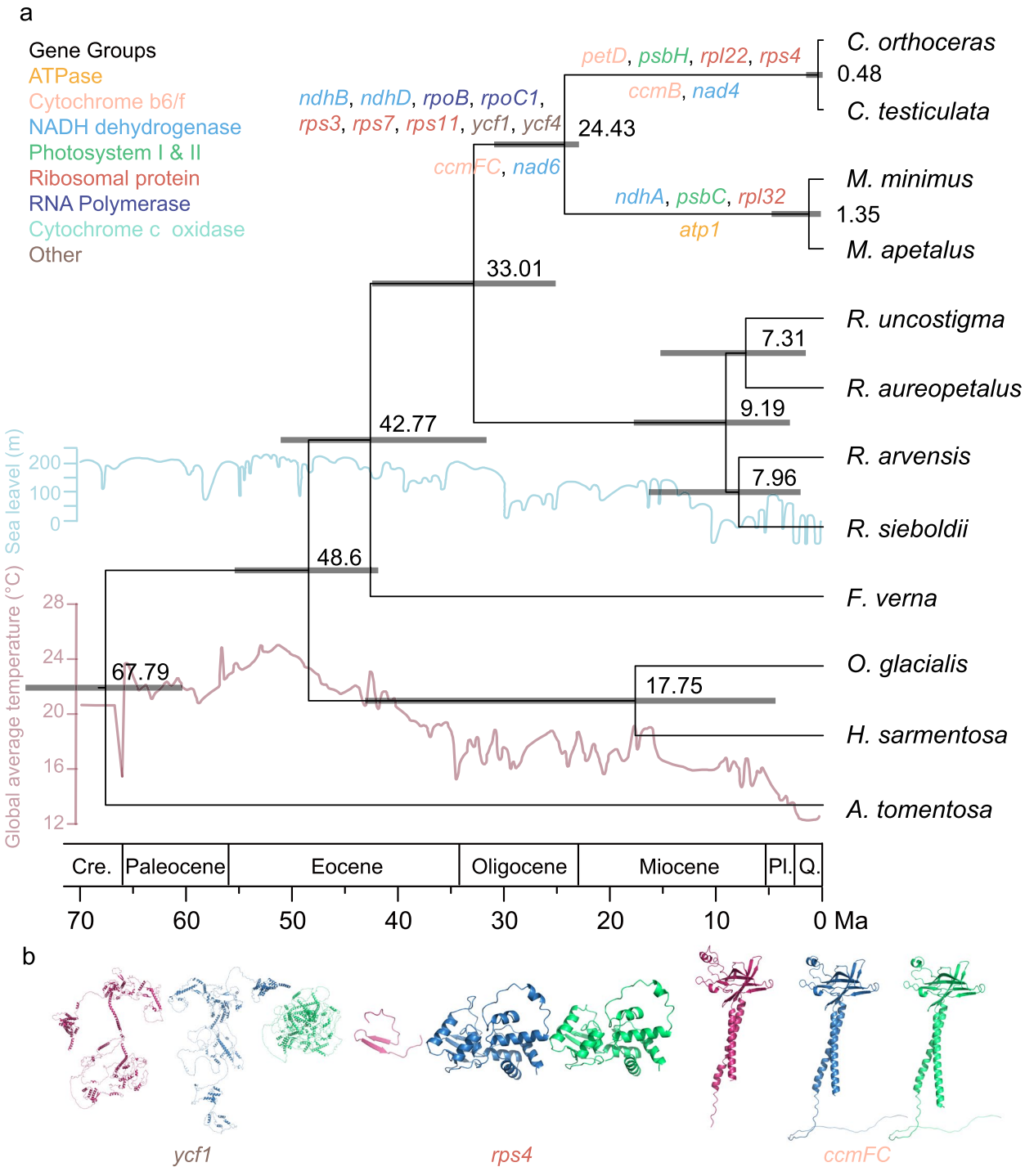

Fig. 3 Chronogram of Ranunculeae and the adaptive evolution of organelle genes. **a** Combined chronogram and evolutionary rate analysis. Dating analysis was performed using BEAST based on the 78-pt gene dataset. The grey bars represent 95% highest posterior density intervals. Plastid and mitochondrial FSGs that were identified were labeled above and below branches, respectively. The depictions of temperature and sea level changes are modified from Scotese et al. [22] and Haq et al. [23], respectively. **b** The predicted protein tertiary models obtained for two FSGs shared by *Ceratocephala* and *Myosurus*, plastid *ycf1* and mitochondrial *ccmFC*, and one FSG in *Ceratocephala*, plastid *rps4*. M2, first major glacial event in the NH; FSGs, fast evolving genes. Cre., Cretaceous; P., Pliocene; Q., Quaternary

two-ratio model (m2) was identified as best-fit. For the cytochrome *c* oxidase gene (*cox1*) and the ribosome large subunit gene (*rpl5*), the one-ratio model (m0) was identified as best-fit (Table S5). The ω values of 6 mt-genes in *Ceratocephala* and 6 mt-genes in *Myosurus* were higher than those in *Ranunculus* (Fig. 2; Table S4). Compared to *Ranunculus*, two genes, i.e. the Cytochrome b_6f complex gene (*ccmFC*) and the NADH dehydrogenase-like complex gene (*nad6*), evolved faster in both *Ceratocephala* and *Myosurus*. Two FSGs, i.e., the Cytochrome b_6f complex gene (*ccmB*) and the NADH dehydrogenase-like complex gene (*nad4*), were identified in *Ceratocephala*. The ATP-Synthase complex gene (*atp1*) was identified to be a FSG in *Myosurus*.

Protein structure model analysis

To structurally characterize the FSGs, we predicted and compared the protein structure of each of the identified FSGs among *Ceratocephala*, *Myosurus*, and *Ranunculus*. For the 8 pt-FSGs shared by *Ceratocephala* and *Myosurus*, sequence identity was generally high among *Ceratocephala*, *Myosurus*, and *Ranunculus*, except for *ycf1* with low sequence identity (< 70%; Table S6; Fig. S5). For the 4 pt-FSGs in *Ceratocephala* and 3 pt-FSGs in *Myosurus*, sequence identity was generally high between *Ceratocephala* and *Ranunculus*, and between *Myosurus* and *Ranunculus*, respectively. Based on template modeling score (TM-score), the predicted protein structure of *ycf1* is markedly different among *Ceratocephala*, *Myosurus*, and *Ranunculus* (< 0.17; Fig. 3; Table S6). The predicted protein structure of *rps4*, a FSG in *Ceratocephala*, is obviously different between *Ceratocephala* and *Ranunculus* (TM-scores < 0.17; Fig. 3; Table S6).

For the 2 mt-FSGs shared by *Ceratocephala* and *Myosurus*, sequence identity was generally high among *Ceratocephala*, *Myosurus*, and *Ranunculus* (> 70%; Fig. S6; Table S7;). For the 2 mt-FSGs in *Ceratocephala* and 1 mt-FSG in *Myosurus*, sequence identity was generally high between *Ceratocephala* and *Ranunculus*, and between *Myosurus* and *Ranunculus*, respectively. Based on TM-scores, the predicted protein structure of *ccmFC*, a FSG shared by *Ceratocephala* and *Myosurus*, is markedly different between *Ceratocephala* and *Myosurus* (< 0.17; Fig. 3; Table S7), and between *Ceratocephala* and *Ranunculus* (< 0.17; Fig. 3; Table S7).

Discussion

Evolutionary rate of organelle genomes in *Ceratocephala* and *Myosurus* lineages

Longer branches in phylogenies usually indicate faster evolutionary rates [20, 21]. Variations in evolutionary rates among lineages (heterotachy) have been widely documented throughout the tree of life [24–26]. The plastomes of maize and rice have faster evolutionary rates than that of tobacco [27]. The plastomes of Poales have faster evolutionary rates than of other commelinid groups [28–30]. The mitogenomes of *Pelargonium* (Geraniaceae) and *Plantago* (Plantaginaceae) have faster evolutionary rates than that of *Silene* (Caryophyllaceae) [31]. The plastome and mitogenome of *Eleocharis* have faster evolutionary rates than those of *Kobresia* in Cyperaceae [27]. All our phylogenomic analyses based on pt- and mt-gene data show that *Ceratocephala* and *Myosurus* formed a clade, sister to *Ranunculus* (Fig. 1), consistent with our previous studies [17–19]. In the pt- and mt-gene trees, the branch lengths of xerophytic *Ceratocephala* and hydrophytic *Myosurus* are longer than the other mesophytic genera of Ranunculeae (Fig. 1), suggesting that the organelle genomes of the two genera may have been evolving at accelerated rates.

The increases in evolutionary rates are probably associated with the specific environment [28]. In Dendrodoridae (Mollusca), the mitogenome of smooth *Dendrodoris* under rocks 0–5 m sea level has faster evolutionary rates than that of warted *Dendrodoris* at 20 m below sea level [29]. In *Cardamine* (Brassicaceae), cold responsive genes in *C. resedifolia* in a high altitude exhibit faster evolutionary rates than *C. impatiens* at a low altitude [7]. Smaller tree ferns living in warmer environments have faster evolutionary rates than other tree ferns [30]. Gillman and Wright [31] proposed that dry and wet environments can affect the evolutionary rates of species. In Ranunculeae, *Ceratocephala* grows in dry habitats, *Myosurus* inhabits wet habitats, whereas other genera of the tribe are mainly distributed in mesophytic habitats. Thus, the accelerated evolutionary rates of *Ceratocephala* and *Myosurus* might be related to their respective adaptation to dry and wet habitats.

FSGs in *Ceratocephala* and *Myosurus*

By comparing two branch models, we identified the two-ratio model as best-fit for 77 pt-genes and 28 mt-genes (Tables S4, S5), which suggests that the majority of organelle genes tend to evolve under a different rate between *Ceratocephala* and *Ranunculus* and between *Myosurus* and *Ranunculus*. The ω values of 37 and 38 organelle protein-coding genes in *Ceratocephala* and *Myosurus* are higher than those in *Ranunculus*, respectively (Fig. 2), implying these genes underwent accelerated evolution. Among the 16 identified FSGs of plastomes in *Ceratocephala* and *Myosurus*, *rps*- and *rpl*-genes are account for a relatively large proportion, and two of the four *rpo*-genes are FSGs. Similar patterns have been found in some taxa. For example, in Geraniaceae *rps*- and *rpl*-genes are highly accelerated [8, 32]; and *rpo*-genes in Annonaceae, Passifloraceae and Geraniaceae are higher evolutionary rates [33, 34]. The *rps*- and *rpl*-genes play a role in light-dependent regulation of transcription/

translation processes [35]. The *rpo*-genes encode plastid-encoded RNA polymerase (PEP), which plays a major role in rRNA synthesis [36]. The mt-FSGs mainly belong to *nad*-genes and *ccm*-genes. In plants, *ccm*-genes acts as a redox sensing hub, pivotal to the regulation of light harvesting and cyclic electron transfer that protect against metabolic and environmental stresses [37].

Nine FSGs in plastome (*ndhB*, *ndhD*, *rpoB*, *rpoC1*, *rps3*, *rps7*, *rps11*, *ycf1*, and *ycf4*) and two FSGs in mitogenome (*ccmFC* and *nad6*) are shared by *Ceratocephala* and *Myosurus* (Fig. 3). Thus, these eleven genes might have been involved in the colonization of new environments by the most recent common ancestor of the two genera, and thereby led to the divergence from the mesophytic sister lineage. Among eleven FSGs, two genes (*ycf1*, *ccmFC*) display genus-specific variations in predicted protein structural features. The plastid gene *ycf1* shows low TM-score in intergeneric comparisons, indicating difference protein structures of this gene among these three genera (Fig. 3; Table S6). The role of *ycf1* has not yet been unambiguously defined [38], but it has been hypothesized to involve the structural remodeling and/or linkage of plastid chromosomes to protein and/or membrane structures [39, 40]. Thus, the structural variation of the predicted protein coded by *ycf1* may be associated with the differentiation of *Ceratocephala* and *Myosurus* to adapt to dry and wet environments, respectively. The mitochondrial gene *ccmFC* shows low TM score in *Ceratocephala* compared to the other two genera, indicating the genus-specific predicted protein structural divergence in *Ceratocephala* (Fig. 3; Tables S7). The *ccmFC* involves in the biogenesis of mitochondrial respiratory complexes III and IV in plants, its protein possesses some conserved domains, especially in the N- and C-terminal parts, and the variation of its structure will have a crucial impact on its function [41]. Thus, the *ccmFC* might have played a significant role in promoting the adaptation of *Ceratocephala* to dry habitats. Whether the structural differences of *ycf1* and *ccmFC* are explicitly linked to adaptation to arid or aquatic environments will be validated by functional experiment in the future.

Our divergence time estimates show that the *Ceratocephala-Myosurus* clade originated in the early Oligocene (33.01 Ma, 95% HPD: 25.26–42.6; Fig. 3). Around the Eocene–Oligocene Transition (EOT, *ca*. 34 Ma), a massive drop in global temperature and a major increase in continental ice volume occurred [42, 43]. Rohde [44] proposed that temperature may change the evolutionary rate of organisms via an influence on the rate of mutagenesis and/or via an indirect influence on rates of selection. The EOT temperature drop might drove both the genus-specific predicted structural divergences in *ycf1* and *ccmFC* proteins and the accelerated evolution of the 11 FSGs shared by *Ceratocephala* and *Myosurus*.

Among the FSGs unique to *Ceratocephala*, the plastid gene *rps4* exhibits distinct predicted protein structural configurations between *Ceratocephala* and *Ranunculus* (Fig. 3; Table S6), suggesting that this gene might have played a potential role in enhancing drought tolerance in *Ceratocephala*. *Ceratocephala* is mainly distributed in Central Asian dry areas with one in New Zealand. The estimated age for the split of *Ceratocephala* and *Myosurus* was at 24.43 Ma (95% HPD: 23.06–31.08; Fig. 3). During this period, the aridification of inland Asia was markedly intensified [45–49]. The uplifts of the Pamir-Tian Shan and the Qinghai-Tibet Plateau [50–53] and the continued retreat of the Paratethys Sea [54–56] might have been main triggers for the climatic change, which led to the expansion of Asian arid ecosystems and consequently drove possibly the evolutionary origin of *Ceratocephala*. Our evolutionary rate analyses identified four pt-FSGs (*petD*, *psbH*, *rpl22*, and *rps4*) and two mt-FSGs (*ccmB* and *nad4*) that were only found in *Ceratocephala* (Fig. 3). Thus, we suggest that these six FSGs and the predicted protein structural difference of *rps4* may be related to the adaptation of *Ceratocephala* to dry habitats in the late Oligocene.

Three pt-FSGs (*ndhA*, *psbC*, and *rpl32*) and one mt-FSG (*atp1*) was only found in *Myosurus* (Fig. 3). *Myosurus* is mainly distributed in wet or seasonally wet areas of all continents. In the late Oligocene (*ca*. 25 Ma), there was a significant rise in global sea level (Fig. 3) [22, 23, 57]. The rise of global sea level may provide wet habitats for *Myosurus*. Thus, we suggest that significant rise in global sea level during the late Oligocene might have promoted the accelerated evolution of the four organelle FSGs in *Myosurus*.

Conclusion

Our integration of phylogenomic, comparative genomic, evolutionary rate, and predicted protein structure variation analyses can be used to explore adaptive evolution of organelle genomes of other plant groups to specific habitats. We show that eleven organelle genes shared by *Ceratocephala* and *Myosurus* underwent accelerated evolution. *Ceratocephala* and *Myosurus* have six and four unique organelle FSGs, respectively. Among these FSGs, the plastid *rpo-*, *rps-* and *rpl-*genes and mitochondrial *nad-* and *ccm-*genes are account for a relatively large proportion, suggesting that they might have played important roles in *Ceratocephala* and *Myosurus* to adapt arid and aquatic habitats, respectively. Additionally, the predicted protein structures of *ycf1*, *rps4* and *ccmFC* in *Ceratocephala* and *Myosurus* were changed, which might have been associated with habitat shifts in the late Oligocene. These findings suggest that FSGs may exhibit habitat-specific functional traits in plant adaptation to arid and aquatic environments. To better understand

the correlation between accelerated evolution rates of these two genera and their adaptation to specific environments, evolutionary rates of nuclear genes need to be investigated in the future since the nuclear genome contains the vast majority of functional genes. In particular, other omics data with larger sample sizes (e.g., transcriptomics and genomics) can be used to validate whether the identified FSGs and predicted protein structure changes drove environmental adaptation of *Ceratocephala* and *Myosurus*.

Materials and methods

Sample sequencing, data assembly, and annotation

We sampled two species of *Ceratocephala* and *Myosurus*, respectively (Fig. S1). Following Wang et al. [16–18, 58], Ranunculeae contains two major clades. For the clade containing *Ceratocephala* and *Myosurus*, we also sampled four mesophytic species of *Ranunculus* and one mesophytic species of *Ficaria*. For the other clade, two mesophytic species from *Halerpestes* and *Oxygraphis* were also included (Table S1). Based on the results of previous studies [18, 59], *Anemone* of Anemoneae, sister to Ranunculeae, was selected as outgroup. Vouchers were deposited in Herbarium, Institute of Botany, Chinese Academy of Sciences, Beijing (PE). Wei Wang and Andrey S. Erst undertook their formal identification. No specific permissions or licenses were required for our collections and experiments. Voucher information and GenBank accession number of plastomes are listed in Table S1. The plastid and mitochondrial gene sequence alignments that were used to generate phylogenetic trees were deposited in the FigShare database (https://doi.org/10.6084/m9.figshare.28957142).

Genomic DNA of the 12 sampled species were extracted from silica gel-dried leaves or herbarium specimens and purified using the Tiangen Isolation/Extraction/Purification Kit (Tiangen Biotech (Beijing) Co., Ltd.). Short insert of 300–500 bp libraries were prepared for sequencing on the Illumina HiSeq X-Ten platform.

The plastome was de novo assembled using GetOrganelle v1.7.6.1 [60] and was annotated by PGA [61] and OGDRAW v1.3.1 (Table S1) [60]. We preliminary extracted 40-mt genes using hybpiper v2.1.6 [62], MitoFinder v1.4.1 [63], and SPAdes v3.15.2 [64]. The amino acid sequences of 78-pt and 40-mt genes were separately aligned in MAFFT v7 [65]. DNA sequences were then aligned using PAL2NAL v14 [66]. We analyzed the values of GC and length of 78-pt and 40-mt genes, then we used the median value to represent each genus.

Phylogenetic analyses and divergence time estimation

The 78-pt genes and 40-mt genes were concatenated separately, and then performed ML analysis using RAxML v8.2.12 [67] with 1,000 replicates under the GTRGAMMA model. Following the suggestion by Wang et al. [17], the thresholds BS ≥ 70% was used as an indication of strongly supported incongruence.

Due to the limited number of mitochondrial genes obtained, divergence times were estimated based on the concatenated 78-pt gene dataset using BEAST v2.1.3 [68]. Fossil achenes of *Myosurus* sp. were found from the Oligocene [69]. The split of *Ceratocephala* and *Myosurus* was thus set at 23.03 Ma, with a lognormal distribution (Fig. S3). The offset (minimum age constraint) was set to be equal to the age of the fossil. The 95% upper bound of the distribution (soft maximum) was set by adjusting the standard deviation with 1.25. The 95% upper bound of the distribution (soft maximum) was determined by adjusting the standard deviation to 1.25. We also used two second calibration points, based on the ages estimated in the recent study [18]: the crown group age of Ranunculeae was constrained at 49.4 Ma (95% HPD: 42.71–55.60) and the root age was constrained at 68.95 Ma (95% HPD: 60.01–74.64; Fig. S3). The standard deviations for these two calibrations are 3.5 and 3.7, respectively, based on a prior normal distribution. An uncorrelated lognormal relaxed clock model of rate variation across branches was used to estimate the divergence time, together with a Yule prior, and the GTR substitution model for each gene partition separately.

The Markov chain Monte Carlo (MCMC) ran for 100,000,000 generations, with sampling every 2,000 generations. We evaluated the convergence using Tracer v1.7.1 [70]. After 25% burn-in, we used TreeAnnotator v1.7.2 [68] to generate the maximum clade credibility (MCC) tree with mean ages and 95% HPD intervals on nodes. We used FigTree v1.4.0 (http://tree.bio.ed.ac.uk/software/figtree/) to generate the chronogram.

Ancestral habitat reconstruction

We first downloaded georeferenced specimen occurrence data of *Ceratocephala* and *Myosurus* from Global Biodiversity Information Facility (GBIF; http://www.gbif.org) . After removing the localities without accurate coordinates, we then dotted the obtained occurrence records into the annual precipitation map that was generated by the WorldClim (www.worldclim.org) at 30-s resolution. We designated each species as xerophytic, mesophytic, or hydrophytic based on aridity index (AI) that was obtained from the Global Aridity Index and Potential Evapo-Transpiration Database v3.1 [71]. Following the criterion of the World Atlas drylands [72], we defined areas with AI of less than 0.20 (encompassing hyper-arid and arid environments) as xerophytic, with AI of more than 0.65 (humid environments) as hydrophytic, and with AI of 0.2–0.65 as mesophytic. Our results show that *Ceratocephala* is xerophytic, *Myosurus* is hydrophytic, and the sampled species from other Ranunculeae and

Anemoneae are mesophytic (Table S1), which are consistent with the descriptions of Tamura [15].

To infer the habitat evolution in Ranunculeae, we optimized habitat type onto the ML tree recovered from the 78-pt gene data using ML approach in Mesquite v2.75 [73]. The Markov k-state one-parameter model of evolution for discrete unordered characters [74] was used.

Evolutionary rate estimation

We ran the one-ratio branch model and two-ratio branch model with CODEML program in PAML v4.9 [75] to estimate the ω, respectively. Partial genes lacking *Ceratocephala* and *Myosurus* were excluded.

We compared two branch models, H0: the one-ratio model (m0) that assumes all branches have been evolving at the same rate (null hypothesis), and HA: the two-ratio model (m2) allows the foreground branch to evolve under a different rate (alternative hypothesis). *Ceratocephala* and *Myosurus* were designated as foreground branches. We used a likelihood ratio test (LRT) to test each model's fit and compare the one-ratio branch and the two-ratio branch models. If a gene had a higher ω in the foreground branch than in the background branch and also had a p-value < 0.05, it was considered as a FSG in the foreground branch. The abnormal ω values ($\omega < 0.001$ or $\omega > 5$) were excluded from our analysis [76, 77].

Protein structure models prediction

For FSGs, we predicted and compared their protein structures in *Ceratocephala* and *Myosurus* using SWISSMODEL [78], with *Ranunculus* as homolog protein template. For each sequence, we kept the structure with the best Global Model Quality Estimate (GMQE) score as reference for our protein structure model [78]. To evaluate the predicted protein structural differences, we evaluated the percentage of sequence similarity, and the topological similarity of the predicted protein structures, known as template modeling TM-score. TM-score is a metric for assessing the topological similarity of protein structures. TM-score has the value in (0,1), where 1 indicates a perfect match between two structures, scores below 0.17 correspond to randomly chosen unrelated proteins, whereas structures with a score higher than 0.5 assume generally the same fold in SCOP/CATH [79, 80].

Abbreviations

FSGs	Fast-evolving genes
plastome	Plastid genome
mitogenome	Mitochondrial genome
pt	Plastid
mt	Mitochondrial
BS	Bootstrap support
ML	Maximum likelihood
TM-scores	Template Modeling Score
HPD	Highest posterior density
EOT	Eocene–Oligocene Transition
PEP	Plastid-encoded RNA polymerase
MCMC	Markov chain Monte Carlo
MCC	Maximum clade credibility
GBIF	Global Biodiversity Information Facility
AI	Aridity index
LRT	Likehood Ratio Test
GMQE	Global Model Quality Estimate

Supplementary Information

The online version contains supplementary material available at https://doi.org/10.1186/s12870-025-08009-0.

Additional file 1: Fig. S1. Geographic distribution of Ceratocephala and Myosurus superimposed on the map of annual precipitation. Fig. S2. Gene contents of plastome and mitogenome. Fig. S3. Chronogram of Ranunculeae based on the 78-pt gene dataset. Fig. S4. Ancestral habitat reconstruction of Ranunculeae. Fig. S5. The predicted protein tertiary structures of fast-evolving genes in plastome. Fig. S6. The predicted protein tertiary structures of fast-evolving genes in mitogenome.

Additional file 2: Table S1. Taxon, voucher, locality, aridity index, and GenBank accession number for the plastome sequences in this study. Table S2. Summary of plastid gene features in Ceratocephala, Myosurus and Ranunculus. Table S3. Summary of mitochondrial gene features in Ceratocephala, Myosurus and Ranunculus. Table S4. Summary of m0 and m2 models that analyzed plastomes in the study. Table S5. Summary of m0 and m2 models that analyzed mitogenomes in the study. Table S6. Pairwise comparison of the predicted plastomic protein structure models. Table S7. Pairwise comparison of the predicted mitochondrial protein structure models.

Authors' contributions

WW and KLX planned and designed the research; HWP, TVE and ASE collected samples; XPZ contributed to data analysis; JL and KLX analyzed the data; WCH, XPZ and GLC revised and provided comments. JL, KLX, ASE and WW wrote the paper. All authors read and approved the manuscript.

Funding

This research was partially funded by the National Natural Science Foundation of China (32400182 and 32361133549), the National Key Research and Development Program of China (2023YFF0805800 and 2024YFF1701404), the Beijing Natural Science Foundation (5244047), the Chinese Academy of Sciences President's International Fellowship Initiative (2025PVA0116 and 2025PVC0060), the Russian Science Foundation (24-44-00027), the state assignments performed by the CSBG SB RAS (AAAA-A21-121011290024-05), the state assignments performed by the ICG SB RAS (FWNR-2025-0020), and the state assignments performed by the SFSCA RAS (075-00563-25-02).

Data availability

Plastomes used in this study are available in the National Center for Biotechnology Information (NCBI) (https://www.ncbi.nlm.nih.gov/nuccore/), with GenBank accession numbers (PV621856-PV621862) shown in Table S1. Plastid and mitochondrial gene sequence alignments used to generate phylogenetic trees are available at the FigShare database (https://doi.org/10.6084/m9.figshare.28957142).

Declarations

Ethics approval and consent to participate

We complied with all relevant institutional, national and international guide lines with permissions from Institute of Botany, Chinese Academy of Sciences. No materials from animal or human were used in this research.

Consent for publication

Not applicable.

Competing interests

The authors declare no competing interests.

Author details
[1]State Key Laboratory of Plant Diversity and Specialty Crops, Institute of Botany, Chinese Academy of Sciences, Beijing 100093, China
[2]University of Chinese Academy of Sciences, Beijing 100049, China
[3]China National Botanical Garden, Beijing 100093, China
[4]Shenzhen Branch, Guangdong Laboratory of Lingnan Modern Agriculture, Genome Analysis Laboratory of the Ministry of Agriculture and Rural Affairs, Agricultural Genomics Institute at Shenzhen, Chinese Academy of Agricultural Sciences, Shenzhen 518120, China
[5]Institute of Cytology and Genetics, Siberian Branch of Russian Academy of Sciences, Novosibirsk 630090, Russia
[6]Siberian Federal Scientific Centre of Agrobiotechnologies of the Russian Academy of Sciences (SFSCA RAS), Krasnoobsk 630501, Russia
[7]Central Siberian Botanical Garden, Siberian Branch of Russian Academy of Sciences, Zolotodolinskaya Str. 101, Novosibirsk 630090, Russia

Received: 21 May 2025 / Accepted: 17 December 2025
Published online: 22 December 2025

References

1. Dong W, Xu C, Wen J, Zhou S. Evolutionary directions of single nucleotide substitutions and structural mutations in the chloroplast genomes of the family Calycanthaceae. BMC Evol Biol. 2020;20:96.
2. Dong S, Li X, Liu Q, Zhu T, Tian A, Chen N, et al. Comparative genomics uncovers evolutionary drivers of locust migratory adaptation. BMC Genomics. 2025;26:203.
3. Young R, Mitterboeck TF, Loeza-Quintana T, Adamowicz S. Rates of molecular evolution and genetic diversity in European vs. North American populations of invasive insect species. Eur J Entomol. 2018;115:718–28.
4. Peoples N, Burns MD, Mihalitsis M, Wainwright PC. Evolutionary lability of a key innovation spurs rapid diversification. Nature. 2025;639:962–7.
5. Harrison TL, Stinchcombe JR, Frederickson ME. Elevated rates of molecular evolution genome-wide in mutualist legumes and rhizobia. Mol Biol Evol. 2024;41:msae245.
6. Orr HA. The genetic theory of adaptation: a brief history. Nat Rev Genet. 2005;6:119–27.
7. Ometto L, Li MA, Bresadola L, Varotto C. Rates of evolution in stress-related genes are associated with habitat preference in two *Cardamine* lineages. BMC Evol Biol. 2012;12:7.
8. Guisinger MM, Kuehl JV, Boore JL, Jansen RK. Genome-wide analyses of Geraniaceae plastid DNA reveal unprecedented patterns of increased nucleotide substitutions. Proc Natl Acad Sci USA. 2008;105:18424–9.
9. Nabholz B, Glémin S, Galtier N. Strong variations of mitochondrial mutation rate across mammals—the longevity hypothesis. Mol Biol Evol. 2008;25:120–30.
10. Medina NS, Moreno-Carmona M, Canal NA, Prada-Quiroga CF. Mitochondrial genome variations and possible adaptive implications in some tephritid flies (Diptera, Tephritidae). Int J Mol Sci. 2025;26:5560.
11. Wang J, Kan S, Liao X, Zhou J, Tembrock LR, Daniell H, et al. Plant organellar genomes: much done, much more to do. Trends Plant Sci. 2024;29:754–69.
12. Wicke S, Schneeweiss GM, dePamphilis CW, Müller KF, Quandt D. The evolution of the plastid chromosome in land plants: gene content, gene order, gene function. Plant Mol Biol. 2011;76:273–97.
13. Yisilam G, Liu Z, Turdi R, Chu Z, Luo W, Tian X. Assembly and comparative analysis of the complete mitochondrial genome of *Isopyrum anemonoides* (Ranunculaceae). PLoS ONE. 2023;18:e0286628.
14. Liu F, Fan W, Yang J-B, Xiang CL, Mower JP, Li DZ, et al. Episodic and guanine–cytosine-biased bursts of intragenomic and interspecific synonymous divergence in Ajugoideae (Lamiaceae) mitogenomes. New Phytol. 2020;228:1107–14.
15. Ranunculaceae TM. In: Hiepko P, editor. Die Natürlichen Pflanzenfamilien, vol. 17a IV. Berlin: Duncker and Humblot; 1995. p. 223–555.
16. Emadzade K, Lehnebach C, Lockhart P, Hörandl E. A molecular phylogeny, morphology and classification of genera of Ranunculeae (Ranunculaceae). Taxon. 2010;59:809–28.
17. Wang W, Li HL, Xiang XG, Chen ZD. Revisiting the phylogeny of Ranunculeae: implications for divergence time estimation and historical biogeography. J Syst Evol. 2014;52:551–65.
18. Wang W, Lin L, Xiang XG, Ortiz Rdel C, Liu Y, Xiang KL, et al. The rise of angiosperm-dominated herbaceous floras: Insights from Ranunculaceae. Sci Rep. 2016;6:27259.
19. Long J, He WC, Peng HW, Erst AS, Wang W, Xiang KL. Comparative plastome analysis of the sister genera *Ceratocephala* and *Myosurus* (Ranunculaceae) reveals signals of adaptive evolution to arid and aquatic environments. BMC Plant Biol. 2024;24:202.
20. Omilian AR, Taylor DJ. Rate acceleration and long-branch attraction in a conserved gene of cryptic daphniid (Crustacea) species. Mol Biol Evol. 2001;18:2201–12.
21. Yang Z. On the best evolutionary rate for phylogenetic analysis. Syst Biol. 1998;47:125–33.
22. Scotese C, Song H, Mills B, van der Meer D. Phanerozoic paleotemperatures: The earth's changing climate during the last 540 million years. Earth-Sci Rev. 2021;215:103503.
23. Haq BU, Hardenbol J, Vail PR. Chronology of fluctuating sea levels since the triassic. Science. 1987;235:1156–67.
24. Stenøien HK. Slow molecular evolution in 18S rDNA, *rbcL* and *nad5* genes of mosses compared with higher plants. J Evol Biol. 2008;21:566–71.
25. Gillman LN, Keeling DJ, Ross HA, Wright SD. Latitude, elevation and the tempo of molecular evolution in mammals. Proc Biol Sci. 2009;276:3353–9.
26. Lanfear R, Ho SY, Jonathan Davies T, Moles AT, Aarssen L, Swenson NG, et al. Taller plants have lower rates of molecular evolution. Nat Commun. 2013;4:1879.
27. Gaut BS, Muse SV, Clegg MT. Relative rates of nucleotide substitution in the chloroplast genome. Mol Phylogenet Evol. 1993;2:89–96.
28. Lanfear R, Welch JJ, Bromham L. Watching the clock: studying variation in rates of molecular evolution between species. Trends Ecol Evol. 2010;25:495–503.
29. Galià-Camps C, Schell T, Enguídanos A, Pegueroles C, Arnedo M, Ballesteros M, et al. Jumping through hoops: Structural rearrangements and accelerated mutation rates on Dendrodoridae (Mollusca: Nudibranchia) mitogenomes rumble their evolution. Mol Phylogenet Evol. 2024;201:108218.
30. Barrera-Redondo J, Ramírez-Barahona S, Eguiarte LE. Rates of molecular evolution in tree ferns are associated with body size, environmental temperature, and biological productivity. Evolution. 2018;72:1050–62.
31. Gillman LN, Wright SD. Species richness and evolutionary speed: the influence of temperature, water and area. J Biogeogr. 2014;41:39–51.
32. Weng ML, Ruhlman TA, Jansen RK. Plastid-nuclear interaction and accelerated coevolution in plastid ribosomal genes in Geraniaceae. Genome Biol Evol. 2016;8:1824–38.
33. Blazier JC, Ruhlman TA, Weng ML, Rehman SK, Sabir JS, Jansen RK. Divergence of RNA polymerase α subunits in angiosperm plastid genomes is mediated by genomic rearrangement. Sci Rep. 2016;6:24595.
34. Zhang X, Sun Y, Landis JB, Lv Z, Shen J, Zhang H, et al. Plastome phylogenomic study of Gentianeae (Gentianaceae): widespread gene tree discordance and its association with evolutionary rate heterogeneity of plastid genes. BMC Plant Biol. 2020;20:340.
35. Sharma MR, Dönhöfer A, Barat C, Marquez V, Datta PP, Fucini P, et al. PSRP1 is not a ribosomal protein, but a ribosome-binding factor that is recycled by the ribosome-recycling factor (RRF) and elongation factor G (EF-G). J Biol Chem. 2010;285:4006–14.
36. Börner T, Aleynikova AY, Zubo YO, Kusnetsov VV. Chloroplast RNA polymerases: role in chloroplast biogenesis. Biochim Biophys Acta. 2015;1847:761–9.
37. Tikhonov AN. The cytochrome b_6f complex: Biophysical aspects of its functioning in chloroplasts. Subcell Biochem. 2018;87:287–328.
38. Bock R. Structure, function, and inheritance of plastid genomes. In: Bock R, editor. Cell and Molecular Biology of Plastids, vol. 19. Springer, Berlin, Heidelberg: Topics in Current Genetics; 2007. p. 29–63.
39. Wolfe KH. Similarity between putative ATP-binding sites in land plant plastid ORF2280 proteins and the FtsH/CDC48 family of ATPases. Curr Genet. 1994;25:379–83.
40. Boudreau E, Turmel M, Goldschmidt-Clermont M, Rochaix JD, Sivan S, Michaels A, et al. A large open reading frame (orf1995) in the chloroplast DNA of *Chlamydomonas reinhardtii* encodes an essential protein. Mol Gen Genet. 1997;253:649–53.
41. Giegé P, Rayapuram N, Meyer EH, Grienenberger JM, Bonnard G. CcmF(C) involved in cytochrome c maturation is present in a large sized complex in wheat mitochondria. FEBS Lett. 2004;563:165–9.
42. Coxall HK, Wilson PA, Pälike H, Lear CH, Backman J. Rapid stepwise onset of Antarctic glaciation and deeper calcite compensation in the Pacific Ocean. Nature. 2005;433:53–7.

43. Westerhold T, Marwan N, Drury AJ, Liebrand D, Agnini C, Anagnostou E, et al. An astronomically dated record of earth's climate and its predictability over the last 66 million years. Science. 2020;369:1383–7.
44. Rohde K. Latitudinal gradients in species diversity: The search for the primary cause. Oikos. 1992;65:514–27.
45. Guo ZT, Ruddiman WF, Hao QZ, Wu HB, Qiao YS, Zhu RX, et al. Onset of Asian desertification by 22 Myr ago inferred from loess deposits in China. Nature. 2002;416:159–63.
46. Sun JM, Ye J, Wu WY, Ni XJ, Bi SD, Zhang ZQ, et al. Late Oligocene-Miocene mid-latitude aridification and wind patterns in the Asian interior. Geology. 2010;38:515–8.
47. Qiang XK, An ZS, Song YG, Chang H, Sun YB, Liu WG, et al. New eolian red clay sequence on the western Chinese Loess Plateau linked to onset of Asian desertification about 25 Ma ago. Sci China Earth Sci. 2011;54:136–44.
48. Rea DK. The paleoclimatic record provided by eolian deposition in the deep sea: The geologic history of wind. Rev Geophys. 1994;32:159–95.
49. Zheng H, Wei X, Tada R, Clift PD, Wang B, Jourdan F, et al. Late Oligocene-early Miocene birth of the Taklimakan Desert. Proc Natl Acad Sci USA. 2015;112:7662–7.
50. Ding L, Spicer RA, Yang J, Xu Q, Cai F, Li S, et al. Quantifying the rise of the Himalayas orogen and implications for the South Asian monsoon. Geology. 2017;45:215–8.
51. Ding L, Kapp P, Cai F, Garzione CN, Xiong Z, Wang H, et al. Timing and mechanisms of Tibetan Plateau uplift. Nat Rev Earth Environ. 2022;3:652–67.
52. Fan B, Liu M, He Z, Meng G, Wu H, Li L. Mesozoic-Cenozoic tectonic evolution and uplift in Pamir: application of fission track thermochronology. Acta Geol Sin. 2021;95:780–93.
53. Jing H, Wang W, Zhang P, Wang Y, Pang J, Zhang Y, et al. Multi-stage uplift and propagation of the Chinese East Tianshan during the Cenozoic. Tectonics. 2025;44:e2024TC008666.
54. Liu XD, Dong BW. Influence of the Tibetan Plateau uplift on the Asian monsoon-arid environment evolution. Chin Sci Bull. 2013;34:4277–91.
55. Hrbek T, Meyer A. Closing of the Tethys Sea and the phylogeny of Eurasian killifishes (Cyprinodontiformes: Cyprinodontidae). J Evol Biol. 2003;16:17–36.
56. Zhang ZS, Wang HJ, Guo ZT, Jiang DB. What triggers the transition of palaeoenvironmental patterns in China, the Tibetan Plateau uplift or the Paratethys Sea retreat? Palaeogeogr Palaeoclimatol Palaeoecol. 2007;245:317–31.
57. Miller KG, Browning JV, Schmelz WJ, Kopp RE, Mountain GS, Wright JD. Cenozoic sea-level and cryospheric evolution from deep-sea geochemi-cal and continental margin records. Sci Adv. 2020;6:eaaz1346.
58. Wang W, Hu H, Xiang XG, Yu SX, Chen ZD. Phylogenetic placements of *Calathodes* and *Megaleranthis* (Ranunculaceae): evidence from molecular and morphological data. Taxon. 2010;59:1712–20.
59. Zhai W, Duan XS, Zhang R, Guo CC, Li L, Xu GX, et al. Chloroplast genomic data provide new and robust insights into the phylogeny and evolution of the Ranunculaceae. Mol Phylogenet Evol. 2019;135:12–21.
60. Jin JJ, Yu WB, Yang JB, Song Y, dePamphilis CW, Yi TS, et al. Getorganelle: a fast and versatile toolkit for accurate de novo assembly of organelle genomes. Genome Biol. 2020;21:241.
61. Qu XJ, Moore MJ, Li DZ, Yi TS. PGA: a software package for rapid, accurate, and flexible batch annotation of plastomes. Plant Methods. 2019;15:50.
62. Johnson MG, Gardner EM, Liu Y, Medina R, Goffinet B, Shaw AJ, et al. HybPiper: Extracting coding sequence and introns for phylogenetics from high-throughput sequencing reads using target enrichment. Appl Plant Sci. 2016;4:apps.1600016.
63. Allio R, Schomaker-Bastos A, Romiguier J, Prosdocimi F, Nabholz B, Delsuc F. Mitofinder: efficient automated large-scale extraction of mitogenomic data in target enrichment phylogenomics. Mol Ecol Resour. 2020;20:892–905.
64. Bankevich A, Nurk S, Antipov D, Gurevich AA, Dvorkin M, Kulikov AS, et al. SPAdes: a new genome assembly algorithm and its applications to single-cell sequencing. J Comput Biol. 2012;19:455–77.
65. Katoh K, Toh H. Parallelization of the MAFFT multiple sequence alignment program. Bioinformatics. 2010;26:1899–900.
66. Suyama M, Torrents D, Bork P. PAL2NAL: Robust conversion of protein sequence alignments into the corresponding codon alignments. Nucleic Acids Res. 2006;34:W609–12.
67. Stamatakis A. RAxML version 8: A tool for phylogenetic analysis and post-analysis of large phylogenies. Bioinformatics. 2014;30:1312–3.
68. Bouckaert R, Heled J, Kühnert D, Vaughan T, Wu CH, Xie D, et al. BEAST 2: a software platform for Bayesian evolutionary analysis. PLoS Comput Biol. 2014;10:e1003537.
69. Mai DH, Walter H. Die Floren der Haselbacher Serie im WeißelsterBecken (Bezirk Leipzig, DDR). Abh Staatl Mus Mineral Geol Dresden. 1978;28:1–200.
70. Rambaut A, Drummond AJ, Xie D, Baele G, Suchard MA. Posterior summarization in bayesian phylogenetics using Tracer 1.7. Syst Biol. 2018;67:901–4.
71. Zomer RJ, Xu J, Trabucco A. Version 3 of the Global Aridity Index and Potential Evapotranspiration Database. Sci Data. 2022;9:409.
72. Middleton NJ, Thomas DSG. World atlas of desertification. 2nd ed. New York: Edward Arnold; 1997.
73. Maddison WP, Maddison DR. Mesquite: A modular system for evolutionary analysis, version 3.10; 2015. http://mesquiteproject.org.
74. Lewis PO. A likelihood approach to estimating phylogeny from discrete morphological character. Syst Biol. 2001;50:913–25.
75. Yang Z. PAML 4: phylogenetic analysis by maximum likelihood. Mol Biol Evol. 2007;24:1586–91.
76. Hu RY, Li XD, Hu Y, Zhang RJ, Lv Q, Zhang M, et al. Adaptive evolution of the enigmatic Takakia now facing climate change in Tibet. Cell. 2023;186:3558–76.
77. Chen L, Qiu Q, Jiang Y, Wang K, Lin Z, Li Z, et al. Large-scale ruminant genome sequencing provides insights into their evolution and distinct traits. Science. 2019;364:eaav6202.
78. Waterhouse A, Bertoni M, Bienert S, Studer G, Tauriello G, Gumienny R, et al. SWISS-MODEL: Homology modelling of protein structures and complexes. Nucleic Acids Res. 2018;46:W296–303.
79. Zhang Y, Skolnick J. Scoring function for automated assessment of protein structure template quality. Proteins. 2004;57:702–10.
80. Xu J, Zhang Y. How significant is a protein structure similarity with TM-score = 0.5? Bioinformatics. 2010;26:889–95.

Publisher's Note